



Full Length Article

Comparative Efficacy of Biogenic Silver Nanoparticles Synthesized by *Pseudochrobactrum* spp. C5 and Chemically Synthesized Silver Nanoparticles for Catalytic Degradation of Methylene Blue and 4-Nitrophenol Dyes

Khadija Siddique¹, Sabir Hussain^{1*}, Muhammad Shahid², Tanvir Shahzad¹, Faisal Mahmood¹, Omer Sadak³, Sundaram Gunasekaran⁴, Tahseen Kamal⁵ and Ikram Ahmad^{6*}

¹Department of Environmental Sciences & Engineering, Government College University Faisalabad, Faisalabad 38000, Pakistan

²Department of Bioinformatics & Biotechnology, Government College University Faisalabad, Faisalabad 38000, Pakistan

³Department of Electrical and Electronics Engineering, Ardahan University, 75000, Turkey

⁴College of Agricultural and Life Sciences, University of Wisconsin-Madison, Wisconsin 53706, United States of America

⁵Department of Chemistry, King Abdul Aziz University, Jeddah, Saudi Arabia

⁶Department of Chemistry, University of Sahiwal, Sahiwal, Pakistan

*For Correspondence: sabirghani@gmail.com; drikramahmad@uosahiwal.edu.pk

Received 21 August 2020; Accepted 24 September 2020; Published 10 December 2020

Abstract

In this study, a novel bacterial strain, *Pseudochrobactrum* spp. C5, was isolated from a wastewater sample and characterized for synthesis of the silver nanoparticles (Ag-NPs). The physicochemical and catalytic properties of biogenic Ag-NPs synthesized by involving the strain C5 were compared with the Ag-NPs synthesized by a chemical reaction. The both types of Ag-NPs were characterized for optical properties by UV-visible spectroscopy and fourier-transform infrared spectroscopy (FT-IR), whereas, the morphological, structural, chemical and electronic state properties were evaluated by field emission scanning electron microscope (FESEM), X-ray diffraction (XRD) and X-ray photoelectron spectroscopy (XPS). These analyses indicated that biogenic Ag-NPs were nano-rod shaped particles ranging from 100–200 nm in size, whereas the chemical Ag-NPs were agglomerated flower shaped structures ranging from 120–300 nm in size. Both types of Ag-NPs were observed to have negative zeta potential values with -27.43 mV and -25.45 mV zeta potential for biogenic and chemically synthesized Ag-NPs. The comparison of both types of Ag-NPs revealed the presence of relatively higher metallic silver (Ag⁰) contents, larger available surface for pollutant's contact and larger distribution of particles in biogenic Ag-NPs as compared to chemically synthesized Ag-NPs, which served for higher catalytic activity. The biogenic Ag-NPs exhibited significantly higher photocatalytic activity for degradation of methylene blue and 4-nitrophenol dyes as compared with that of chemically synthesized Ag-NPs. The findings of this study suggest that the biological Ag-NPs synthesized by *Pseudochrobactrum* spp. C5 might serve as a potential green solution for treatment of dyes loaded textile wastewaters. © 2021 Friends Science Publishers

Keywords: Microbial synthesis; *Pseudochrobactrum* spp.; Silver nanoparticles; Photocatalysis; Methylene blue and 4-nitrophenol

Introduction

Nanotechnology is a vast field dealing with nano sized particles. The nanoparticles have unique size dependent physicochemical properties that give them privilege of an exclusive class to be used as catalyst in numerous products. Shapes and features of surfaces, size, opto-nanomechanical spectroscopic properties and nanoscale compositional mapping define the performance of these heterogeneous catalysts (Korhonen *et al.* 2007; Tasbihi *et al.* 2007). Silver

nanoparticles (Ag-NPs) are the most commonly synthesized materials being studied for different applications such as plant disease control, photonics, electronics, anti-pathogenic and therapeutic activities and catalytic degradation of synthetic dyes (Hu and Chan 2004; Habouti *et al.* 2010; Joseph and Mathew 2015; Wei *et al.* 2015). The Ag-NPs are produced by various methods which might be based on chemical, physical and biological processes (Abid *et al.* 2002; Kalimuthu *et al.* 2008; Nadagouda *et al.* 2011).

Chemical synthesis normally involves the chemical

reduction of silver salts by using a reducing agent (Bankura *et al.* 2012). However, biological synthesis of nanoparticles has nowadays gained a considerable interest of the scientific community because of being an eco-friendly approach that gives different sizes and shapes with no or limited use of harmful solvents (Maurer-Jones *et al.* 2009; Marquis *et al.* 2009; Love *et al.* 2012; Sharifi *et al.* 2012; Schrofel *et al.* 2014). Biological systems are also economic options for nanoparticle fabrication due to their least requirement of energy (Pearce *et al.* 2008). For example, bacteria with their unique property of metal reduction are considered as a potential bio-resource for nanoparticles synthesis (Shantkriti and Rani 2014; Noman *et al.* 2020). The resistance of the bacteria to extreme environmental conditions makes them a favourable candidate for synthesis of such materials (Rouch *et al.* 1995; Lee *et al.* 2019). *Pseudomonas stutzeri* AG 259 (isolated from silver mines) was the first bacterial strain reported for the possibility of nanoparticle synthesis by using microbial machinery (Haefeli *et al.* 1984). In that study, a silver nitrate solution added with bacterial strain provided 200 nm sized, equilateral triangles and hexagons nanoparticle that were fixed within the bacterial cells (Joerger *et al.* 2000). Up till now different bacteria including *Streptomyces atrovirens*, *Shewanella oneidensis* MR-1 strain and *Bacillus* strain CS have been reported for synthesis of Ag-NPs (Song and Shi 2017; Subbaiya *et al.* 2017).

Industrialization is an important sector which is playing a vital role in world economy. However, rapid industrialization has led to introduction of enormous quantities of different types of pollutants including the synthetic organic dyes into the environment (Imran *et al.* 2015). For instance, textile industries release massive quantities of wastewaters which are loaded with different types of contaminants including the synthetic dyes (Sharma and Anamika 2008; Imran *et al.* 2015). Some of the studies reported that 15–50% of the dye stuff used during textile processing is released in textile wastewaters without any treatment (Bisschops and Spanjers 2003; Carmen and Daniela 2012; Imran *et al.* 2015). The presence of dyes in textile wastewaters negatively affects the quality of aquatic and soil resources as well as the health of various living organisms including the human beings (Imran *et al.* 2015, 2019). Hence, untreated dyes loaded wastewaters are a burning issue that needs to be addressed with immediate actions to save groundwater quality and different forms of life on earth (Dulkadiroglu *et al.* 2002).

The use of nanoparticles for catalytic degradation of synthetic dyes has nowadays gained a considerable attention worldwide (Jiang *et al.* 2009; Sheikh *et al.* 2016). Nanoscale size and increased band gap are favourable qualities for redox reactions and, hence, nanoparticles are now in extensive use for dyes removal from textile wastewaters (Di *et al.* 2009; Noman *et al.* 2020). Different types of nanoparticles such as titanium dioxide, zinc oxide, copper and magnesium oxide nanoparticles have been reported for

degradation of different synthetic dyes (Gozmen *et al.* 2009; Moussavi and Mahmoudi 2009; Khataee *et al.* 2015; Noman *et al.* 2020). However, Ag-NPs have gained considerable importance due to its electron relay effect between donor and acceptor (Mallick *et al.* 2006; Zhou *et al.* 2006). The chemically produced Ag-NPs have also been reported to be used in photocatalytic degradation of synthetic dyes (Edison *et al.* 2016; Mariselvam *et al.* 2016). During the recent years, there is a growing interest in developing the green strategies for pollution control including the wastewater treatment. Biosynthesis of the nanomaterials for their application in different functions including the treatment of wastewaters loaded with synthetic dyes is gaining a considerable interest as a green approach (Song and Shi 2017; Noman *et al.* 2020). However, there is little information about the application of the biogenic Ag-NPs as a catalyst for degradation of dyes.

The present study was conducted to isolate and characterize a novel bacterium, *Pseudochrobactrum* spp. C5, having the potential for synthesis of silver nanoparticles. This biologically produced silver nanomaterial was then characterized through FESEM (Field Emission Scanning Electron Microscopy), FT-IR (Fourier Transform Infrared Spectroscopy), DLS (Dynamic light scattering) technique, XRD (X-ray Diffraction) and XPS (X-ray photoelectron spectroscopy). The characteristics of these biologically synthesized silver nanoparticles were compared with that of the silver nanoparticles produced by chemical process. Catalytic potential of bacterially synthesized and chemically synthesized silver nanoparticles was evaluated using methylene blue and 4-nitrophenol as target synthetic dyes.

Materials and Methods

Isolation of the strain C5

Isolation of the Ag-NPs synthesizing bacterial strain was carried out from a textile wastewater sample collected from Khurrianwala, Faisalabad. Isolation of the bacterial colonies was carried out following a serial dilution of the wastewater sample in mineral salt medium as already reported by Hussain *et al.* (2020). The purified bacterial isolates were exposed to different concentrations of silver (50 to 2500 mg L⁻¹), as silver nitrate in mineral salt agar medium for evaluating their tolerance to silver in terms of minimum inhibitory concentration (MIC). The isolates having the high values of MIC of silver were tested for silver reduction in mineral salt medium incubated under shaking in dark at 28°C. The most efficient silver tolerant bacterial strain showing the good potential for silver reduction was chosen for the next studies.

Identification of the strain C5

Identification of the Ag-NPs producing selected bacterial isolate was carried out through amplification, sequencing

and analysis of its 16S rDNA gene using 27f and 1492r primers according to the method already reported by Hussain *et al.* (2013). The sequence was analysed through NCBI Blast and by constructing a phylogenetic tree as already reported by Hussain *et al.* (2013). The sequence was submitted in GeneBank Database under accession number MT318655.

Biosynthesis of nanoparticles

The strain C5 was cultured in 50 mL nutrient broth (NB) medium at 28°C under shaking (150 rpm) overnight. After 24 h incubation, the culture of C5 was tested for its potential of Ag-NPs synthesis. For this purpose, 0.003 M silver was used for 50 mL of bacterial growth culture. After adding the silver salt, all the samples were kept under shaking at 150 rpm at 28°C. At the end of the reaction time (24 h), the culture was collected and kept at 85°C for drying. The dried product was collected and kept in muffle furnace at 700°C for 7 h to get it calcinated.

Chemical synthesis of nanoparticles

The Ag-NPs were chemically synthesized by reducing the metal salt. In a typical experiment, 0.5 M solution of silver nitrate was slowly hydrolyzed by adding 0.5 M NaOH (Qamar *et al.* 2015). Solution mixture was stirred and heated constantly until a brown colour was appeared. A fine powder of precipitates was collected by calcination as already described above.

Characterizations of nanoparticles

UV-visible spectra of synthesized Ag-NPs were recorded on Lambda 25, PerkinElmer spectrometer and FT-IR spectroscopy was done with PerkinElmer Spectrum-100 FT-IR spectrometer (FTIR-Bruker TENSOR-27). The zeta potential was estimated by a dynamic light scattering technique (Zeta PALS, Brookhaven Instrument Corp., Holtsville, N.Y., U.S.A.) and particle size distribution profile was studied using Dynamic light scattering (DLS) technique, whereas, morphology was evaluated by FESEM (FESEM, LEO 1530-1). X-ray Diffraction (PANalytical X'PERT PRO) was used to identify phase transitions by using CuK-alpha radiations (Lambda= 0.1542 nm, 40 kV, 20 mA) and Elemental composition was determined by X-ray photoelectron spectroscopy (Thermo scientific K Alpha instrument).

Photocatalytic potential of nanoparticles

The catalytic activity of the biogenic and the chemically synthesized Ag-NPs was observed by testing them for degradation of two selected synthetic dyes *viz.*, methylene blue (MB) and 4-nitrophenol (4-NP). For this purpose, 1

mM aqueous solutions of each of MB, 4-NP and NaBH₄ were prepared. For catalytic degradation of MB, the treatments consisted of MB added with NaBH₄ (Control treatment), MB added with NaBH₄ along with biogenic Ag-NPs (T₁) and MB added with NaBH₄ along with chemically synthesized Ag-NPs (T₂). The experiment was conducted in three replicates under completely randomized arrangement. For each treatment of this experiment, ¾ of 1 mM MB solution was added with ¼ of 1 mM NaBH₄ solution and distributed in nine cuvettes (Three cuvettes for each treatment). The control treatment consisted of the three cuvettes containing only the combined solution of MB and NaBH₄. For the treatment T₁, 10 mg of the biogenic Ag-NPs in powdered form were added to each of the three cuvettes containing the combined solution of MB and NaBH₄. For the treatment T₂, 10 mg of the chemically synthesized Ag-NPs in powdered form were added to each of the three cuvettes containing the combined solution of MB and NaBH₄. All the cuvettes were stirred constantly for 5 min and kept in natural light to complete the reaction. At different time intervals over the incubation period, the aliquots were taken, centrifuged (10000 rpm for 5 min) and the supernatants were scanned at different wavelength from 500 to 800 nm using the Perkin Elmer UV-Vis spectroscope (U.S.A.) to monitor the degradation of MB. The similar treatments and procedure were followed for the experiment carried out for 4-NP degradation in which all the reagents and conditions were kept the same except that 1 mM 4-NP solution was used instead of 1 mM MB solution. The centrifuged solutions of 4-NP were scanned at different wavelength from 200 to 600 nm using the Perkin Elmer UV-Vis spectroscope (USA) to monitor the degradation of 4-NP. The incubation and scanning were carried out until the both solutions were almost completely decolorized.

Over 60 min incubation period, aliquots were taken from all the replicates of each sample, centrifuged (10000 rpm for 5 min) and analyzed at 668 nm (λ_{max}) for methylene blue and 405 nm (λ_{max}) for 4-Nitrophenol using the Perkin Elmer UV-Vis spectroscope (U.S.A.). Decolorization was calculated as below:

$$\text{Decolorization}(\%) = \frac{X - Y}{X} \times 100$$

Where X and Y represents the control without any treatment and the sample with treatment, respectively.

Statistical analysis

One way analysis of variance (ANOVA) was performed to determine the significance of the treatment effects on decolorization of methylene blue and 4-Nitrophenol separately. Tukey's HSD test was used for multiple means comparisons for decolorization (%) for all the treatments. The statistical analysis was performed using Statistix 8.1.

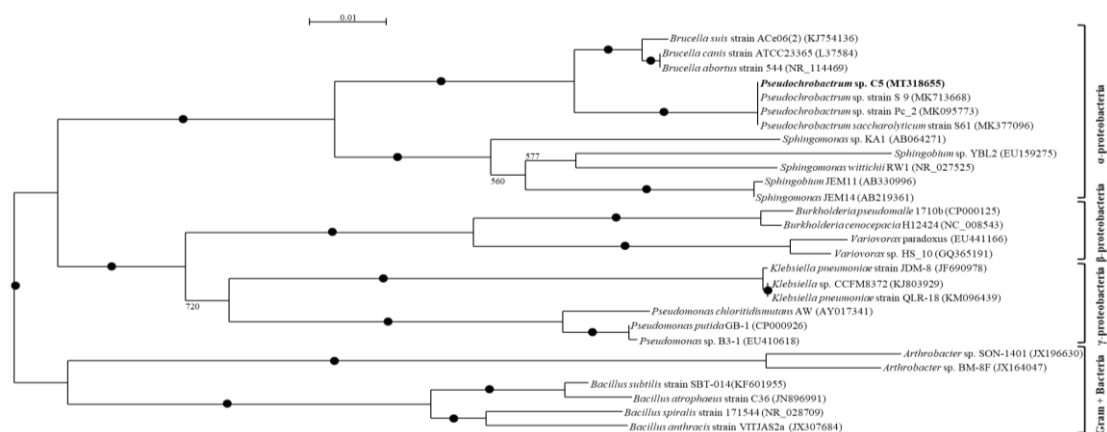


Fig. 1: Neighbour joining phylogenetic tree of *Pseudochrobactrum* spp. C5

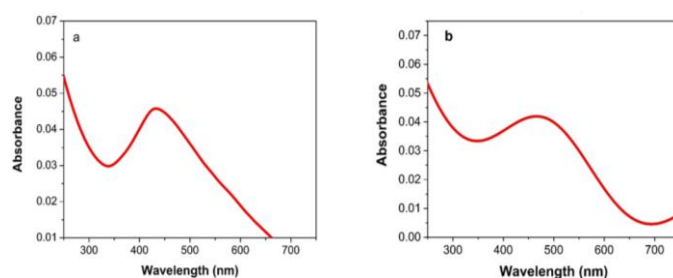


Fig. 2: The comparison of absorption spectra of biosynthesized (a) and chemically synthesized (b) Ag-NPs

Results

Screening and identification of silver nanoparticles producing bacterium

In this study, 28 different types of bacteria having varying colony types and shapes were isolated and purified from the wastewater. All the isolated bacteria were separately tested for MIC of silver by letting them grow at varying concentrations of silver ($50\text{--}2500\text{ mg L}^{-1}$) on mineral salt agar media plates. The isolates showed varying levels of tolerance to the presence of silver in the medium. Out of these tested 28 bacterial colonies, four bacterial isolates (C3, C5, C17, C23) were found to resist the presence of even 2500 mg L^{-1} of silver in the medium. These selected four silver tolerant bacterial isolates were tested for synthesis of nanoparticle. On the basis of the silver tolerance and the synthesis of nanoparticles, the isolate C5 was chosen for next studies. The analysis of 16S rDNA gene of this strain on BlastN indicated that this strain belonged to genus *Pseudochrobactrum*. The phylogenetic analysis also indicated that this strain was grouped with the bacterial strain belonging to genus *Pseudochrobactrum* (Fig. 1). Based on BlastN and phylogenetic analyses, it was designated as *Pseudochrobactrum* spp. C5 (GeneBank Accession No. MT318655).

Different concentrations of silver were tested for synthesis of its nanoparticle by the strain

Pseudochrobactrum. The concentration of 800 mg L^{-1} of silver was selected for synthesis of nanoparticles because an efficient synthesis of prominent brown coloured Ag-NPs by *Pseudochrobactrum* spp. C5 was detected at this concentration under the set conditions.

Characterization of silver nanoparticles

Collective oscillations of free electrons in resonance with light wave were detected by UV analyser. Highest absorbance peaks were observed at 430 nm in case of biosynthesized Ag-NPs (Fig. 2a) and a sharp peak was observed at 420 nm in case of chemically synthesized Ag-NPs (Fig. 2b). To check the zeta potential, charge and polarity of Ag-NPs, both the materials were dispersed in distilled water and sonicated for 5 min to break the bonds between the particles. A dynamic light scattering analyser characterized the illuminations of de-aggregated molecules by a laser beam. Both the materials showed negative ZP values. In case of biologically synthesized Ag-NPs, the average ZP value was -27.43 mV (Fig. 3a) while chemically synthesized Ag-NPs showed -25.54 mV ZP value (Fig. 3b).

The FT-IR analysis provided the idea about interaction between the protein structures and Ag-NPs. Very small amount of dried powder of nanoparticles were analysed on Perkin Elmer one IR spectrophotometer within the range of $500\text{ to }4000\text{ cm}^{-1}$. The spectra of biologically produced Ag-NPs in the range of $500\text{ to }4000$ showed many sharp peaks

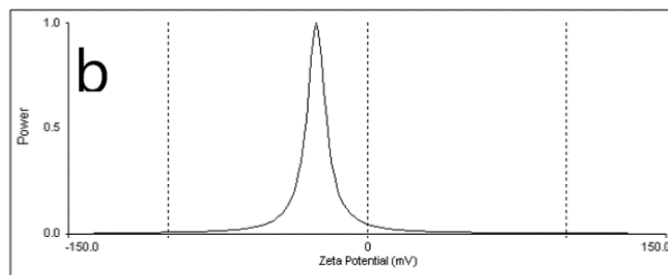


Fig. 3: The comparison of zeta-potential profiles of biosynthesized (a) and chemically synthesized (b) Ag-NPs

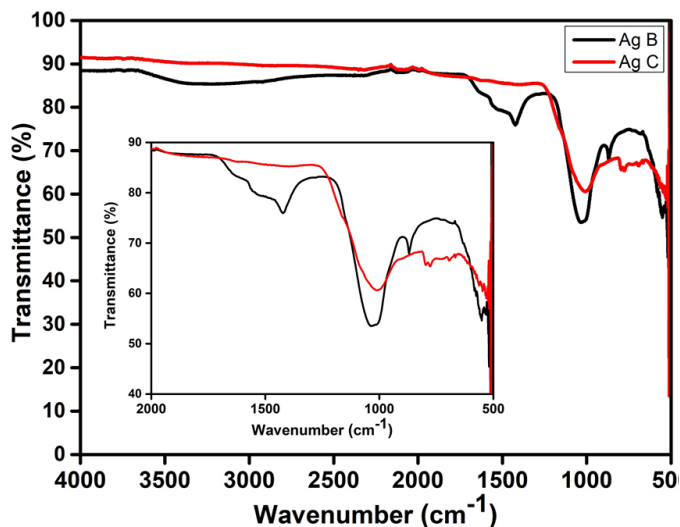


Fig. 4: The comparison of FT-IR spectra of biosynthesized (Ag B) and chemically synthesized (Ag C) silver nanoparticles. The inset figure is the exploded view of the same from 500 to 2000 cm^{-1}

at 3372 cm^{-1} , 2117 cm^{-1} , 1989 cm^{-1} , 1646 cm^{-1} , 1534 cm^{-1} , 1421 cm^{-1} , 1034 cm^{-1} , 869 cm^{-1} and 553 cm^{-1} (Fig. 4). The FT-IR spectra of chemically produced Ag-NPs (Fig. 4) showed sharp peaks at 3452 cm^{-1} , 3043 cm^{-1} , 2893 cm^{-1} , 2827 cm^{-1} , 1677 cm^{-1} , 1627 cm^{-1} , 1435 cm^{-1} , 1373 cm^{-1} , 1055 cm^{-1} and 1007 cm^{-1} respectively.

The morphology of both chemically and biologically synthesized Ag-NPs was estimated by FESEM. The results indicated the agglomeration of chemically synthesized Ag-NPs with a flower like shape and 120–300 nm in size (Fig. 5a, b), while the biologically synthesized Ag-NPs were 100–200 nm in size and nano-rod like shape (Fig. 5c, d). The phase formations of both Ag-NPs were examined with the XRD analysis. Both the chemically produced and biogenic Ag-NPs showed characteristic peaks of Ag-NPs at $2\theta = 38.3^\circ$, 44.2° , 64.5° , 77.5° , 33.3° and 47.6° (Fig. 6a, b).

The XPS analysis was carried out to compare and investigate the chemical compositions of chemically and biologically synthesized Ag-NPs. High resolution 3d spectra in Fig. 7 showed peaks at 374.3 and 368.3 eV for chemically synthesized Ag-NPs while biologically synthesized Ag-NPs showed a peak shift from 374.3, 368.3 eV to 374.8, 368.8 eV.

Photocatalytic degradation studies

Absorption spectra of both the methylene blue and 4-nitrophenol showed a constant decrease in peaks for both dyes at different time breaks as shown in Fig. 8. There was an obvious trend of low absorption peaks as exposure time with catalyst increased. The methylene blue has a broad peak at 666 nm and there was a slight shift of λ_{max} with addition of NaBH_4 that is considered to be a strong reducing agent (Fig. 8a). The slight shift is observed due to dilution effect and there was no further decrease in position even after 30 min. The UV-Visible spectral data of 1 mM methylene blue solution that was treated against $\frac{1}{4}$ of NaBH_4 and 10 mg of biological Ag-NPs has been presented in Fig. 8b. There was a constant decrease in peak intensity after addition of biosynthesized catalyst and it just took 18 min of duration to fully degrade the methylene blue (Fig. 8b) while chemically synthesized Ag-NPs degraded the same volume of methylene blue in 180 min (Fig. 8c).

In case of 4-NP, a maximum absorption peak was observed at 400 nm and a slight shift of λ_{max} was also observed after 150 min due to dilution effect (Fig. 8d). There was a constant decrease in peak intensity after

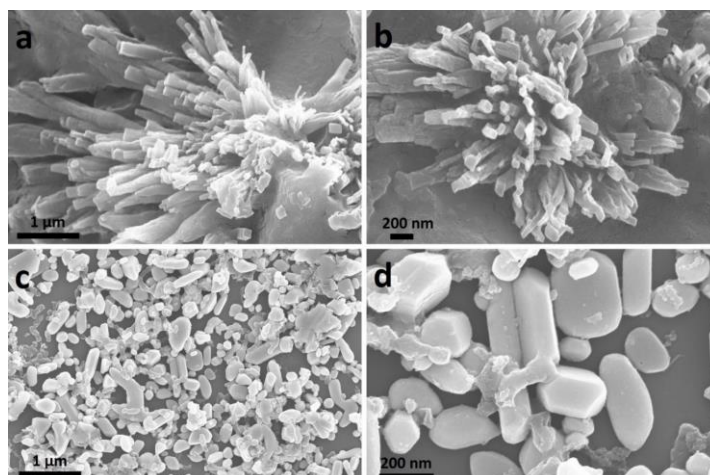


Fig. 5: The comparison FESEM images of chemically synthesized (a & b) and biosynthesized (c & d) Ag-NPs at different magnifications

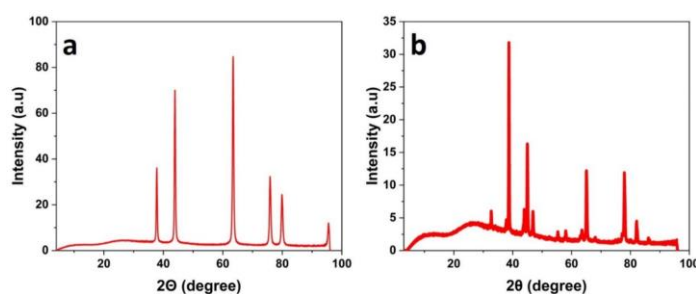


Fig. 6: The comparison of XRD spectra of chemically synthesized (a) and biosynthesized (b) Ag-NPs

addition of biological Ag-NPs catalyst. The formation of 4-AP was observed in 70 min when treated with biological Ag-NPs catalyst (Fig. 8e) while chemically synthesized Ag-NPs catalyst performed the same function in 140 min (Fig. 8f). Absorption kinetics of MB and 4-NP by biosynthesized and chemically synthesized Ag NPs are shown in Fig. 9.

The results clearly indicated that, over a 60 min incubation period, the catalytic decolorization of both the methylene blue and 4-nitrophenol was significantly higher in the treatments where the biogenic Ag-NPs were used as a catalyst as compared to the treatments where chemically synthesized Ag-NPs were used (Fig. 10).

Discussion

In the present study, the Ag-NPs producing *Pseudochrobactrum* spp. C5 was isolated from the textile wastewater. The bacterial culture was initially light yellow in colour before the addition of silver salt that eventually started turning to brown with the addition of silver and the colour was more intense with the passage of time. The specific brown colour was an indication of silver nanoparticle formation as it has already been described in a number of previous such studies (Joerger *et al.* 2000;

Kalimuthu *et al.* 2008; Manivasagan *et al.* 2013). Despite that few bacterial strains belonging to different genera have been reported for synthesis of various nanoparticles (Subbaiya *et al.* 2017; Song and Shi 2017; Noman *et al.* 2020), to the best of our knowledge, there is not even a single report regarding the synthesis of nanoparticles from the bacterial strains belonging to the genus *Pseudochrobactrum*. Hence, *Pseudochrobactrum* spp. C5 might be a novel potential bioresource for biosynthesis of nanoparticles.

Biosynthesis of Ag-NPs by the strain C5 was further confirmed by UV-Visible spectral analysis of the nanoparticles in which specific peaks were observed at wavelengths of 430 nm (Fig. 2a) and 420 nm (Fig. 2b) as indicator of specific brown colour as already previously reported by Sondi and Salopek-Sondi (2004). The stability of the Ag-NPs was determined by their zeta potential values because a nano-suspension with zeta potential values within the range of ± 30 mV is supposed to be a stable suspension (Shameli *et al.* 2012). The zeta potential values of the biogenic and chemically synthesized Ag-NPs were ranging between -25.54 mV and -27.43 mV (Fig. 3), respectively, pointing towards a physical stability of both types of Ag-NPs due to inter-particle repulsions.

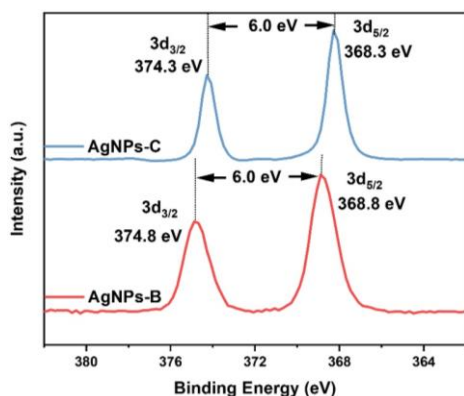


Fig. 7: The comparison of High resolution XPS spectra of Ag 3d for chemically and biological synthesized Ag-NPs. AgNPs-C and AgNPs-B represent the chemically and biologically synthesized Ag-NPs, respectively

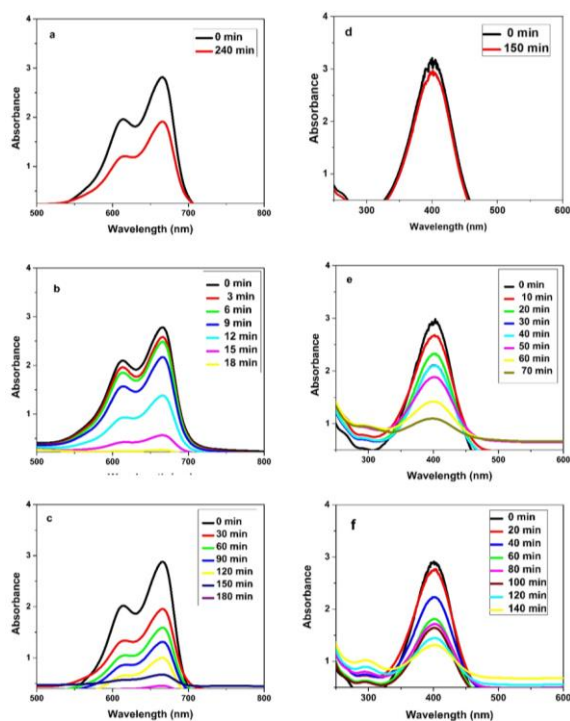


Fig. 8: The comparison of degradation of methylene blue in presence of NaBH_4 (a), NaBH_4 and biosynthesized Ag-NPs (b) and NaBH_4 and chemically synthesized Ag-NPs (c) as well as the degradation of 4-nitrophenol in the presence of NaBH_4 (d), NaBH_4 and biosynthesized Ag-NPs (e) and NaBH_4 and chemically synthesized Ag-NPs (f). The absorbance spectra have been prepared on the basis of mean values having the coefficient of variation values ranging from 1.2 to 9.7 %

The FT-IR analyses of the Ag-NPs showed different characteristic peaks for both types of nano-particles which represented different functional groups (Fig. 4). In case of biogenic Ag-NPs (Fig. 4), a sharp peak around 3372 cm^{-1} represented secondary amides (N-H stretching, H-bond).

Another peak at 2117 cm^{-1} indicated alkyne bond stretching. The peak at 1989 cm^{-1} represented C-O stretching, the peak at 1646 cm^{-1} represented C=C stretching, the peaks at 1534 cm^{-1} and 1421 cm^{-1} represented C-C stretching, the peaks at 1034 cm^{-1} , 869 cm^{-1} indicated C-O stretching and the peak at 553 cm^{-1} indicated =C-H bending (Phanjom and Ahmed 2015). The FT-IR spectra of chemically produced Ag-NPs showed sharp peaks at 3452 cm^{-1} and 3043 cm^{-1} which were indication of amino group stretching (Fig. 4). Peaks at 2893 cm^{-1} and 2827 cm^{-1} were showing C-H bond stretching, while the peaks at 1677 cm^{-1} and 1627 cm^{-1} were related to amine group stretching. The peaks at 1435 cm^{-1} and 1373 cm^{-1} were showing C=C bond stretching that were specific to aromatic amine group and the peaks at 1055 cm^{-1} and 1007 cm^{-1} were an indication of C=O bond stretching in proteins. Free amine group serves as bonding agents between Ag-NPs and proteins. The FESEM images (Fig. 5) suggested for a relatively smaller particle size of the biogenic Ag-NPs resulting into a relatively higher surface area which might result into a relatively better catalytic activity (Cheng *et al.* 2014). During XRD analysis, the characteristic peaks of Ag-NPs at $2\theta = 38.3^\circ$, 44.2° , 64.5° , 77.5° (Fig. 6) corresponded to (111), (200), (220), and (311) planes, respectively, and the data were matching well with those reports in literature and the joint committee on powder diffraction standards (JCPDS) file No. 04-0783. In addition to these characteristic peaks, biological synthesized Ag-NPs showed unpredicted crystalline structures peaks around $2\theta = 33.3^\circ$ and 47.6° which can be due to carbon-based impurities which might be formed after the calcination at 700°C (Ahmad *et al.* 2012; Pasupuleti *et al.* 2013). As shown in high resolution 3d spectra of Ag-NPs in Fig. 7, the chemically synthesized Ag-NPs showed peaks at 374.3 and 368.3 eV which is corresponding to $3d_{3/2}$ and $3d_{5/2}$, respectively, and separated by 6.0 eV. However, when biologically synthesized Ag-NPs were analysed, the peaks at 374.3 and 368.3 eV shifted to 374.8 and 368.8 eV. The shift in the binding energy is attributed to higher metallic silver (Ag^0) in biologically synthesized Ag-NPs (Gurunathan *et al.* 2014).

The photocatalytic degradation of both the methylene blue and 4-nitrophenol as model dyes was carried out in the presence of sodium borohydride and Ag-NPs to check the catalytic efficiency of both types of synthesized nanomaterials. As the methylene blue is stable in almost all types of environment, it is often considered as a probe pollutant in photocatalytic studies (Kamal *et al.* 2016; Kamal 2019). Relatively faster photocatalytic decolourization of methylene blue in the experiment containing biological Ag-NPs catalyst (Fig. 8) might be due to relatively large surface area, smaller size and dispersion tendency of biological Ag-NPs as compared to that of the chemically synthesized Ag-NPs catalysts (Kamal *et al.* 2016; Ahmad *et al.* 2017). The degradation rate of 4-nitrophenol was slower as compared to that of the

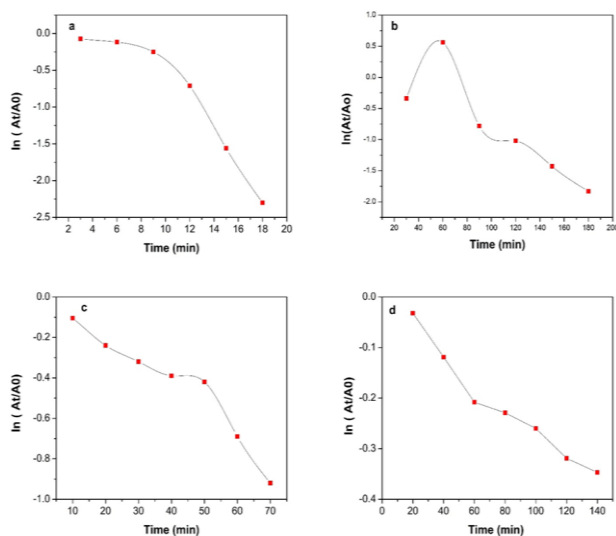


Fig. 9: Plot of $\ln(A_t/A_0)$ Vs Time of MB by biosynthesized (a) and chemically synthesized (b) Ag-NPs and of 4-NP by biosynthesized (c) and chemically synthesized (d) Ag-NPs

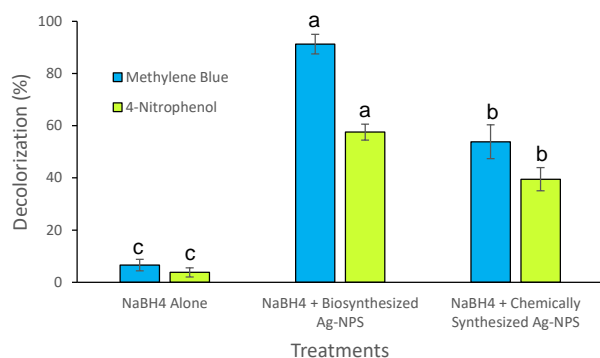


Fig. 10: Catalytic decolorization of methylene blue and 4-Nitrophenol in the presence of different treatments using the biogenic and chemically synthesized Ag-NPs over an incubation period of 60 min

methylene blue in the presence of both types of Ag-NPs (Fig. 8). This might be due to the formation of 4-aminophenol as an end product during the reduction of 4-nitrophenol in the reaction catalysed by Ag-NPs. The kinetic barrier between the donor BH_4^- and acceptor 4-NP^+ was covered by Ag-NPs by lowering activation energy. Once the donor BH_4^- and acceptor 4-NP^+ were absorbed on the surface of Ag-NPs, catalytic reduction took place by transferring the electron from BH_4^- to p-nitrophenolate ion (Khan *et al.* 2016). This conversion might have been achieved by the formation of an intermediate 4-nitrophenolate ion. The faster degradation rate of 4-nitrophenol in presence of biologically synthesized Ag-NPs, used as catalyst, can be better explained in terms of its relatively large surface area, smaller size and dispersion tendency as compared to chemically synthesized Ag-NPs catalysts (Kamal *et al.* 2016; Ahmad *et al.* 2017).

Adsorption kinetics plays a major role in degradation process (Baransi *et al.* 2012). It has been observed that photocatalytic particles adsorb organic components of solution coming on surface from the bulk of material. In the experiment containing biologically synthesized Ag-NPs as catalyst, a slower degradation was observed at the start of the experiment which can be better explained by adsorption kinetics for methylene blue and 4-nitrophenol, respectively (Fig. 9). Once the particles get settled, the biological Ag-NPs catalyst starts working and a fast degradation rate is observed (Fig. 9) as also previously reported by Khan *et al.* (2016). However, in case of the experiments containing chemically synthesized Ag-NPs, a constant pattern of decolorization of both the dyes was observed as can be found in the adsorption kinetics calculated for methylene blue and 4-nitrophenol, respectively. All these findings suggest for higher catalytic efficiency of the biologically synthesized Ag-NPs as compared to the chemically synthesized Ag-NPs. The potential of photocatalytic degradation of synthetic dyes by the biogenic Ag-NPs synthesized by the strain C5 is an important feature which can be exploited for treatment of the coloured textile wastewaters that can be a potential threat to the quality of water that ultimately affects all life forms on earth (Imran *et al.* 2019; Noman *et al.* 2020).

Conclusion

Findings of this study concluded that *Pseudochrobactrum* spp. C5 isolated from a textile wastewater might be a potential candidate for green synthesis of stable Ag-NPs with variable shapes and uniform dispersion. Moreover, it was concluded that biosynthesized Ag-NPs were catalytically more efficient in decolorizing the model dyes methylene blue and 4-nitrophenol as compared to chemically synthesized Ag-NPs. Hence, the Ag-NPs synthesized by *Pseudochrobactrum* spp. C5 might be effectively used for devising the environment friendly green strategies for treatment of wastewaters containing the dyes.

Acknowledgement

The authors acknowledge the 'Department of Environmental Sciences & Engineering, Government College University Faisalabad, Pakistan' and the 'College of Agricultural and Life Sciences, University of Wisconsin-Madison, USA for providing the research facilities for conducting this research. The authors are also grateful to Higher Education Commission (HEC), Pakistan for providing funding under Indigenous PhD Fellowships (Phase II, Batch III) No. 315-3044-2SS3-022/HEC/Sch-Ind/2015.

Author Contributions

KS conducted all the experiments and wrote the first draft of the manuscript. SH and IA were involved in planning and

supervising the experiments as well as final write-up of the manuscript. MS, TS and FM helped in conducting the experiments and in improving the write-up of the manuscript. OS, SG and TK supported in characterization of the nanoparticles as well as in write-up of the manuscript.

References

- Abid JP, A Wark, PF Brevet, H Girault (2002). Preparation of silver nanoparticles in solution from a silver salt by laser irradiation. *Chem Commun* 7:792–793
- Ahmad I, SB Khan, T Kamal, AM Asiri (2017). Visible light activated degradation of organic pollutants using zinc-iron selenide. *J Mol Liq* 229:429–435
- Ahmad N, S Sharma, R Rai (2012). Rapid green synthesis of silver and gold nanoparticles using peels of *Punica granatum*. *Adv Mater Lett* 3:376–380
- Bankura K, D Maity, MM Mollick, D Mondal, B Bhowmick, M Bain, A Chakraborty, J Sarkar, K Acharya, D Chattopadhyay (2012). Synthesis, characterization and antimicrobial activity of dextran stabilized silver nanoparticles in aqueous medium. *Carbohydr Polym* 89:1159–1165
- Baransi K, Y Dubowski, I Sabbah (2012). Synergetic effect between photocatalytic degradation and adsorption processes on the removal of phenolic compounds from olive mill wastewater. *Water Res* 46:789–798
- Bisschops I, H Spanjers (2003). Literature review on textile wastewater characterisation. *Environ Technol* 24:1399–1411
- Carmen Z, S Daniela (2012). *Textile organic dyes—characteristics, polluting effects and separation/elimination procedures from industrial effluents—a critical overview*, Vol. 2741, p:31. Org Pollutants Ten Years After the Stockholm Convention—environ and Anal Update
- Cheng H, J Wang, Y Zhao, X Han (2014). Effect of phase composition, morphology, and specific surface area on the photocatalytic activity of TiO₂ nanomaterials. *RSC Adv* 4:47031–47038
- Di X, SK Kansal, W Deng (2009). Preparation, characterization and photocatalytic activity of flowerlike cadmium sulfide nanostructure. *Sep Purif Technol* 68:61–64
- Dulkadiroglu H, S Dogruel, D Okutman, I Kabdaşlı, S Sözen, D Orhon (2002). Effect of chemical treatment on soluble residual COD in textile wastewaters. *Water Sci Technol* 45:251–259
- Edison TNJI, R Atchudan, MG Sethuraman, YR Lee (2016). Reductive-degradation of carcinogenic azo dyes using *Anacardium occidentale* testa derived silver nanoparticles. *J Photochem Photobiol B Biol* 162:604–610
- Gozmen B, M Turabik, A Hesenov (2009). Photocatalytic degradation of Basic Red 46 and Basic Yellow 28 in single and binary mixture by UV/TiO₂/periodate system. *J Hazard Mater* 164:1487–1495
- Gurunathan S, J Raman, SN Malek, P John, S Vikineswary (2014). Green synthesis of silver nanoparticles using *Ganoderma neo-japonicum* Imazeki: A potential cytotoxic agent against breast cancer cells. *Intl J Nanomed* 8:4399–4413
- Habouti S, CH Solterbeck, M Es-Souni (2010). Synthesis of silver nano-fir-twins and application to single molecules detection. *J Mater Chem* 20:5215–5219
- Haefeli C, C Franklin, KE Hardy (1984). Plasmid-determined silver resistance in *Pseudomonas stutzeri* isolated from a silver mine. *J Bacteriol* 158:389–392
- Hu X, C Chan (2004). Photonic crystals with silver nanowires as a near-infrared superlens. *Appl Phys Lett* 85:1520–1522
- Hussain S, Z Maqbool, M Shahid, T Shahzad, S Muzammil, M Zubair, M Iqbal, I Ahmad, M Imran, M Ibrahim, F Mahmood (2020). Simultaneous removal of reactive dyes and hexavalent chromium by a metal tolerant *Pseudomonas* spp. WS-D/183 harboring plant growth promoting traits. *Intl J Agric Biol* 23:241–252
- Hussain S, Z Maqbool, S Ali, T Yasmeen, M Imran, F Mahmood, F Abbas (2013). Biodecolorization of reactive black-5 by a metal and salt tolerant bacterial strain *Pseudomonas* spp. RA20 isolated from Paharang drain effluents in Pakistan. *Ecotoxicol Environ Saf* 98:331–338
- Imran M, M Ashraf, S Hussain, A Mustafa (2019). Microbial biotechnology for detoxification of azo-dye loaded textile effluents: A critical review. *Intl J Agric Biol* 22:1138–1154
- Imran M, M Arshad, A Khalid, S Hussain, MW Mumtaz, DE Crowley (2015). Decolorization of Reactive Black-5 by *Shewanella* spp. in the Presence of Metal Ions and Salts. *Water Environ Res* 87:579–586
- Jiang R, H Zhu, X Li, L Xiao (2009). Visible light photocatalytic decolorization of CI Acid Red 66 by chitosan capped CdS composite nanoparticles. *Chem Eng J* 152:537–542
- Joerger R, T Klaus, CG Granqvist (2000). Biologically produced silver-carbon composite materials for optically functional thin-film coatings. *Adv Mater* 12:407–409
- Joseph S, B Mathew (2015). Facile synthesis of silver nanoparticles and their application in dye degradation. *Mater Sci Eng B* 195:90–97
- Kalimuthu K, RS Babu, D Venkataraman, M Bilal, S Gurunathan (2008). Biosynthesis of silver nanocrystals by *Bacillus licheniformis*. *Colloid Surf B Biointerf* 65:150–153
- Kamal T (2019). Aminophenols formation from nitrophenols using agar biopolymer hydrogel supported CuO nanoparticles catalyst. *Polym Test* 77:105896
- Kamal T, Y Anwar, SB Khan, MTS Chani, AM Asiri (2016). Dye adsorption and bactericidal properties of TiO₂/chitosan coating layer. *Carbohydr Polym* 148:153–160
- Khan SB, SA Khan, HM Marwani, EM Bakhsh, Y Anwar, T Kamal, AM Asiri, K Akhtar (2016). Anti-bacterial PES-cellulose composite spheres: Dual character toward extraction and catalytic reduction of nitrophenol. *Rsc Adv* 6:110077–110090
- Khataee A, A Karimi, S Arefi-Oskoui, RDC Soltani, Y Hanifehpour, B Soltani (2015). Sonochemical synthesis of Pr-doped ZnO nanoparticles for sonocatalytic degradation of Acid Red 17. *Ultrason Sonochem* 22:371–381
- Korhonen ST, SM Airaksinen, MA Banares, AOI Krause (2007). Isobutane dehydrogenation on zirconia-, alumina-, and zirconia/alumina-supported chromia catalysts. *Appl Catal A Gen* 333:30–41
- Lee NY, WC Ko, PR Hsueh (2019). Nanoparticles in the Treatment of Infections Caused by Multidrug-Resistant Organisms. *Front Pharmacol* 10: Article 1153
- Love SA, MA Maurer-Jones, JW Thompson, YS Lin CL Haynes (2012). Assessing nanoparticle toxicity. *Annu Rev Anal Chem* 5:181–205
- Mallick K, M Witcomb, M Scurrall (2006). Silver nanoparticle catalysed redox reaction: An electron relay effect. *Mater Chem Phys* 97:283–287
- Manivasagan P, J Venkatesan, K Senthilkumar, K Sivakumar, SK Kim (2013). Biosynthesis, antimicrobial and cytotoxic effect of silver nanoparticles using a novel *Nocardia* spp. *MBRC-1. Biomed Res Intl* 2013; Article 287638
- Mariselvam R, A Ranjitsingh, P Mosae Selvakumar, AA Alarfaj, MA Munusamy (2016). Spectral studies of UV and solar photocatalytic degradation of AZO dye and textile dye effluents using green synthesized silver nanoparticles. *Bioinorg Chem Appl* 2016; Article 8629178
- Marquis BJ, SA Love, KL Braun, CL Haynes (2009). Analytical methods to assess nanoparticle toxicity. *Anlnt* 134:425–439
- Maurer-Jones MA, KC Bantz, SA Love, BJ Marquis, CL Haynes (2009). Toxicity of therapeutic nanoparticles. *Nanomed* 4:219–241
- Moussavi G, M Mahmoudi (2009). Removal of azo and anthraquinone reactive dyes from industrial wastewaters using MgO nanoparticles. *J Hazard Mater* 168:806–812
- Nadagouda MN, TF Speth, RS Varma (2011). Microwave-assisted green synthesis of silver nanostructures. *Accounts Chem Res* 44:469–478
- Noman M, M Shahid, T Ahmed, MBK Niazi, S Hussain, F Song, I Manzoor (2020). Use of biogenic copper nanoparticles synthesized from a native *Escherichia* spp. as photocatalysts for azo dye degradation and treatment of textile effluents. *Environ Pollut* 257; Article 113514
- Pasupuleti VR, TNVKV Prasad, RA Shiekh, SK Balam, G Narasimulu, CS Reddy, IA Rahman, SH Gan (2013). Biogenic silver nanoparticles using *Rhinacanthus nasutus* leaf extract: Synthesis, spectral analysis, and antimicrobial studies. *Intl J Nanomed* 8:3355–3364

- Pearce CI, VS Coker, JM Charnock, RA Patrick, JFW Mosselmans, N Law, TR Beveridge, JR Lloyd (2008). Microbial manufacture of chalcogenide-based nanoparticles via the reduction of selenite using *Veillonella atypica*: An *in situ* EXAFS study. *Nanotechnol* 19:1–13
- Phanjom P, G Ahmed (2015). Biosynthesis of silver nanoparticles by *Aspergillus oryzae* (MTCC No. 1846) and its characterizations. *Nanosci Nanotechnol* 5:14–21
- Qamar MT, M Aslam, IM Ismail, N Salah, A Hameed (2015). Synthesis, characterization, and sunlight mediated photocatalytic activity of CuO coated ZnO for the removal of nitrophenols. *ACS Appl Mater Interf* 7:8757–8769
- Rouch DA, BT Lee, AP Morby (1995). Understanding cellular responses to toxic agents: A model for mechanism-choice in bacterial metal resistance. *J Ind Microbiol* 14:132–141
- Schrofel A, G Kratosova, I Safarik, M Safarikova, I Raska, LM Shor (2014). Applications of biosynthesized metallic nanoparticles—a review. *Acta Biomater* 10:4023–4042
- Shantkriti S, P Rani (2014). Biological synthesis of copper nanoparticles using *Pseudomonas fluorescens*. *Intl J Curr Microbiol Appl Sci* 3:374–383
- Sharifi S, S Behzadi, S Laurent, ML Forrest, P Stroeve, M Mahmoudi (2012). Toxicity of nanomaterials. *Chem Soc Rev* 41:2323–2343
- Sharma A, SJ Anamika (2008). Screening of microorganisms for azo dye degradation from dye affected sites of Sanganer, Rajasthan, India. *J Pure Appl Microbiol* 2:365–372
- Sheikh MUD, GA Naikoo, M Thomas, M Bano, F Khan (2016). Solar-assisted photocatalytic reduction of methyl orange azo dye over porous TiO₂ nanostructures. *New J Chem* 40:5483–5494
- Shameli K, MB Ahmad, EA JaffarAlMulla, NA Ibrahim, P Shabanzadeh, A Rustaiyan, Y Abdollahi, S Bagheri, S Abdolmohammadi, MS Usman, M Zidan (2012). Green biosynthesis of silver nanoparticles using *Callicarpa maingayi* stem bark extraction. *Molecules* 17:8506–8517
- Sondi I, B Salopek-Sondi (2004). Silver nanoparticles as antimicrobial agent: A case study on *E. coli* as a model for Gram negative bacteria. *J Colloid Interf Sci* 275:177–182
- Song X, X Shi (2017). Bioreductive deposition of highly dispersed Ag nanoparticles on carbon nanotubes with enhanced catalytic degradation for 4-nitrophenol assisted by *Shewanella oneidensis* MR-1. *Environ Sci Pollut Res* 24:3038–3044
- Subbaiya R, M Saravanan, AR Priya, KR Shankar, M Selvam, M Ovais, R Balajee, H Barabadi (2017). Biomimetic synthesis of silver nanoparticles from *Streptomyces atrovirens* and their potential anticancer activity against human breast cancer cells. *IET Nanobiotechnol* 11:965–972
- Tasbihi M, F Feyzi, M Amlashi, A Abdullah, A Mohamed (2007). Effect of the addition of potassium and lithium in Pt–Sn/Al₂O₃ catalysts for the dehydrogenation of isobutane. *Fuel Proc Technol* 88:883–889
- Wei L, J Lu, H Xu, A Patel, ZS Chen, G Chen (2015). Silver nanoparticles: Synthesis, properties, and therapeutic applications. *Drug Discov Today* 20:595–601
- Zhou WP, A Lewera, R Larsen, RI Masel, PS Bagus, A Wieckowski (2006). Size effects in electronic and catalytic properties of unsupported palladium nanoparticles in electrooxidation of formic acid. *J Phys Chem B* 110:13393–13398